Available online at www.sciencedirect.com

ScienceDirect

Energy Procedia 63 (2014) 5512 – 5521

Energy Procedia

GHGT-12

Laboratory batch experiments and geochemical modelling of water-rock-super critical CO_2 reactions in Gulf of Mexico Miocene rocks: Implications for future CCS projects

Patrick J. Mickler*, Changbing Yang, Jiemin Lu, Kimberly D. Lankford#

Bureau of Economic Geology, The University of Texas at Austin
The Department of Geological Sciences, The University of Texas at Austin

Abstract

Storage of CO_2 in deep saline formations in a super critical liquid state has been proposed as a way to mitigate the effects of increased atmospheric CO_2 levels. The ultimate fate of the CO_2 after injection requires an understanding of mineral dissolution/precipitation reactions occurring between the target formation minerals and the existing formation brines at formation temperatures and pressures in the presence of supercritical CO_2. In this experiment core material taken from a Miocene age Gulf of Mexico core from a depth of 2806 m was reacted with synthetic brine at varied but high temperatures and pressures in the presence of super critical CO_2. XRD and SEM analyses were conducted before and after reaction to identify dissolution of existing minerals and precipitation of authigenic mineral phases. Periodic geochemical analysis of the reaction fluid was used to quantify changes in the elemental composition of the reaction fluid which helps identify potential mineral dissolution/precipitation reactions.

Reaction brine (140 ml) was loaded into a high pressure reaction vessel with 8 g of core sample. Experimental temperature was set to 70, 100 or 130°C; pressure was set to 200 or 300 bar, and solution chemistry was changed from de-ionized (DI) water to a 1.88 M NaCl solution. After the introduction of CO_2 the Ca and alkalinity concentrations showed the largest increases, Ca concentrations increased ~1000 ppm, suggesting carbonate dissolution was the dominant geochemical reaction. Final equilibrium Ca concentrations increased with decreasing reaction temperature because of greater CO_2 solubility. In addition, the reactions with the NaCl brine produced higher equilibrium Ca concentrations than the DI water experiment, likely due to the decrease in ion activity with higher ionic strength solutions. Pressure change from 200 to 300 bar did not significantly alter reaction

* Corresponding author. Tel.: 1-512-232-7125; fax: 1-512-471-0140.
E-mail address: pat.mickler@beg.utexas.edu

Peer-review under responsibility of the Organizing Committee of GHGT-12
doi:10.1016/j.egypro.2014.11.584

rates. Unlike Ca, silicate dissolution reactions appear to be positively correlated with reaction temperature. Silicate dissolution rates are 2 orders of magnitude slower than carbonate dissolution rates.

In this study, PHREEQC was used to simulate brine-rock-CO_2 interactions in batch experiments under high pressure and high temperature. Generally, the geochemical models reproduced concentration of Ca, Mg, K and Si seen in the water rock experiments suggesting that carbonate and K-feldspar dissolution are the dominant geochemical reactions. In addition, geochemical models show that dawsonite precipitates in higher salinity (higher Na+ concentration) experiments.

Peer-review under responsibility of the Organizing Committee of GHGT-12
Keywords:

Introduction:

The capture of CO_2 from point sources including power plants, condensing that CO_2 into a supercritical liquid ($CO_{2\,sc}$), and storing that liquid in deep saline reservoirs have been proposed as a way of reducing atmospheric CO_2 concentrations [1,2]. The ultimate fate of the $CO_{2\,sc}$ is partially dependent upon temperature and pressure controlled mineral dissolution/precipitation reactions occurring between formation brines and formation minerals in the presence of $CO_{2\,sc}$. In this study we will explore likely changes to formation brine chemistry by reacting Miocene age core samples from the offshore Texas coast with manufactured brine in the presence of $CO_{2\,(sc)}$. The offshore Texas coast was chosen for study because of the large local sources of anthropogenic CO_2 and the large volume of Miocene age sands that may be suitable for long term $CO_{2\,(sc)}$ storage. The resulting changes in solution chemistry and comparisons of SEM images and XRD results of pre and post experimental formation minerals were used to identify mineral dissolution/precipitation reactions. Reaction results will be used to refine PHREEQC geochemical models also used to identify mineral dissolution/precipitation reactions affecting elemental concentrations. Changes in aqueous chemistry will also give us insight into the fate of potentially hazardous trace elements, including As, Cr, etc., that exist as trace elements in formation minerals.

Methods:

Autoclave experiments

The autoclave apparatus consists of a stainless steel reaction vessel in which rock fragments, approximately 140 ml of aqueous solution and super critical CO_2 can be reacted at elevated temperatures and pressures. Experimental temperatures were varied between 70°C and 130°C and pressure was varied between 200 and 300 bars. Ports allow for the incremental injection of super-critical CO_2 to maintain pressure and incremental sampling of the liquid phase in the sample chamber without interruption of the experiment. The incremental sampling of the aqueous solution and its subsequent analysis is used to produce a time series of changes in solution chemistry driven by water-rock-super critical CO_2 reactions. Experimental temperature and pressure are maintained by computer control. In these experiments, approximately 8 g of rock sample were reacted with De-ionized water or a 1.88 M NaCl solution (a solution typical of the pore fluid encounter in the offshore Miocene rocks studied).

XRD analysis

Formation mineralogy was quantitatively analyzed using random-powder X-ray diffraction (XRD), [3]. Samples were disintegrated using a TEMA ball mill and then wet-grinded using a McCrone Micronizing Mill. Mineral-water slurry samples were sprayed through the heated chamber of a spray drier, and the spherical droplets of dried powder was collected for analysis. XRD was conducted on a Bruker AXS D8 diffractometer at The University of Texas at Austin (UT), and quantitative analysis was performed using Topas 3, which is PC software

that is based on the Rietveld method [4]. Sample-preparation methods and analytical parameters can be found in [5]. Mineralogy compositions of formation sediments are listed in Table 1

SEM analysis

Rock chips of the unreacted and reacted samples were rinsed in DI water, air dried and coated with iridium before SEM examination. The sample surfaces were examined under secondary electron mode for topography using a field-emission SEM, a FEI Nova NanoSEM 430. Energy-dispersive spectroscopy (EDS) point analyses of specific grains were conducted for mineral identification. Element-distribution maps were also acquired using two EDS detectors. The EDS maps are rendered as false-color images overlying SEM images to show mineralogical variation in the examined area.

Geochemical analysis

Major cations and anions were analyzed on two Dionex ICS-2000 Ion Chromatography systems equipped with auto-eluent generators, an AS-HV auto sampler, and an AD25 Absorbance Detector at UT. Samples were initially diluted with deionized water so that no component would be >100 ppm. Trace elements were analyzed on an Agilent 7500ce quadrupole inductively coupled plasma-mass spectrometer (ICP-MS) at UT. Samples for trace metals were acidified to 2% HNO_3 immediately after collection and diluted so that the total dissolved solid content was close to 500 ppm.

Alkalinity titrations were performed by titrating approximately 2-3 ml of reacted solution, diluted with DI to ~40 ml, with 0.1600 N H_2SO_4 solutions using a Hach digital titrator. The USGS alkalinity calculator was used to determine the alkalinity of the solution using the inflection point method.

Geochemical Modelling

In this study, PHREEQC, was used to simulate brine-rock-CO_2 interactions in batch experiments under high pressure and high temperature [6]. PHREEQC generally is used for performing a wide variety of low-temperature aqueous geochemical calculations. However, it has been used to simulate water-rock-CO_2 interactions under high-pressures and high-temperatures [7-13] as long as an appropriate geochemical database is used.

In this study, geochemical models are based on the integrated LLNL thermodynamic database, ‘‘thermo.com.V8.R6.230’’[14]. The reaction constants compiled in this database can be applied to the temperature ranging from 0^{o}C to 300^{o}C. However, PHREEQC simulates gas phases as ideal gases. It may lead to significant errors if total pressures of the gas phase measured in the batch experiments are directly used in PHREEQC. So in this study, we used WINPROP to calculate CO_2 gas fugacity of each batch experiment as partial pressure of CO_2 in PHREEQC. WINPROP is CMG's equation of state multiphase equilibrium property package featuring fluid characterization, lumping of components, matching of laboratory data through regression, simulation of multiple contact processes, phase diagram construction, solids precipitation, and more [15].

Results

The experiment was allowed to come to temperature and pressure under a Nitrogen atmosphere for a couple days. During this time modest increases in TDS were observed. At experiment time=0, the inert gas atmosphere was replaced by $CO_{2\,(sc)}$. The element Ca, and measured alkalinity, showed the largest increase in concentration and fastest release rates. Plots of the concentration of Ca, Mg, Si and K vs. reaction time with changing experimental temperature are given in Fig. 1. The Ca concentrations increased until they reached equilibrium values and these equilibriums were controlled by temperature and solution chemistry. Higher equilibrium concentrations were reached at lower experimental temperatures and higher solution salinities. Changing experimental pressure did not significantly affect equilibrium Ca concentrations. The elements Mg and Sr

show similar timing of increases in concentration as Ca however the magnitude of the change is lower. Other elements that show significant increases in concentration with reaction time are Si, K and Mn however it does not appear that these elements reach equilibrium in during the reaction time. Small increases in concentration with reaction time were also seen in Ba, P, Co, Rb, Cs, Pb, Fe and Ni. The Fe and Ni are also present in the metallic body of the reaction cell.

The elements Al, Cr, As and Mo show initial enrichment with the addition of $CO_{2\,(sc)}$. The concentration of the elements decreased after the initial mobilization to low values or values below the detection limit of the ICP-MS. Other elements analysed exhibit no consistent trends in concentration over the experimental run. The element B shows the highest concentration of ~14 ppm. Other elements Ti, U, Co, Se, Zr, Cd, Sb, Bi and V show variable concentrations including values below the detection limit of the ICP-MS after the initial increase in concentration.

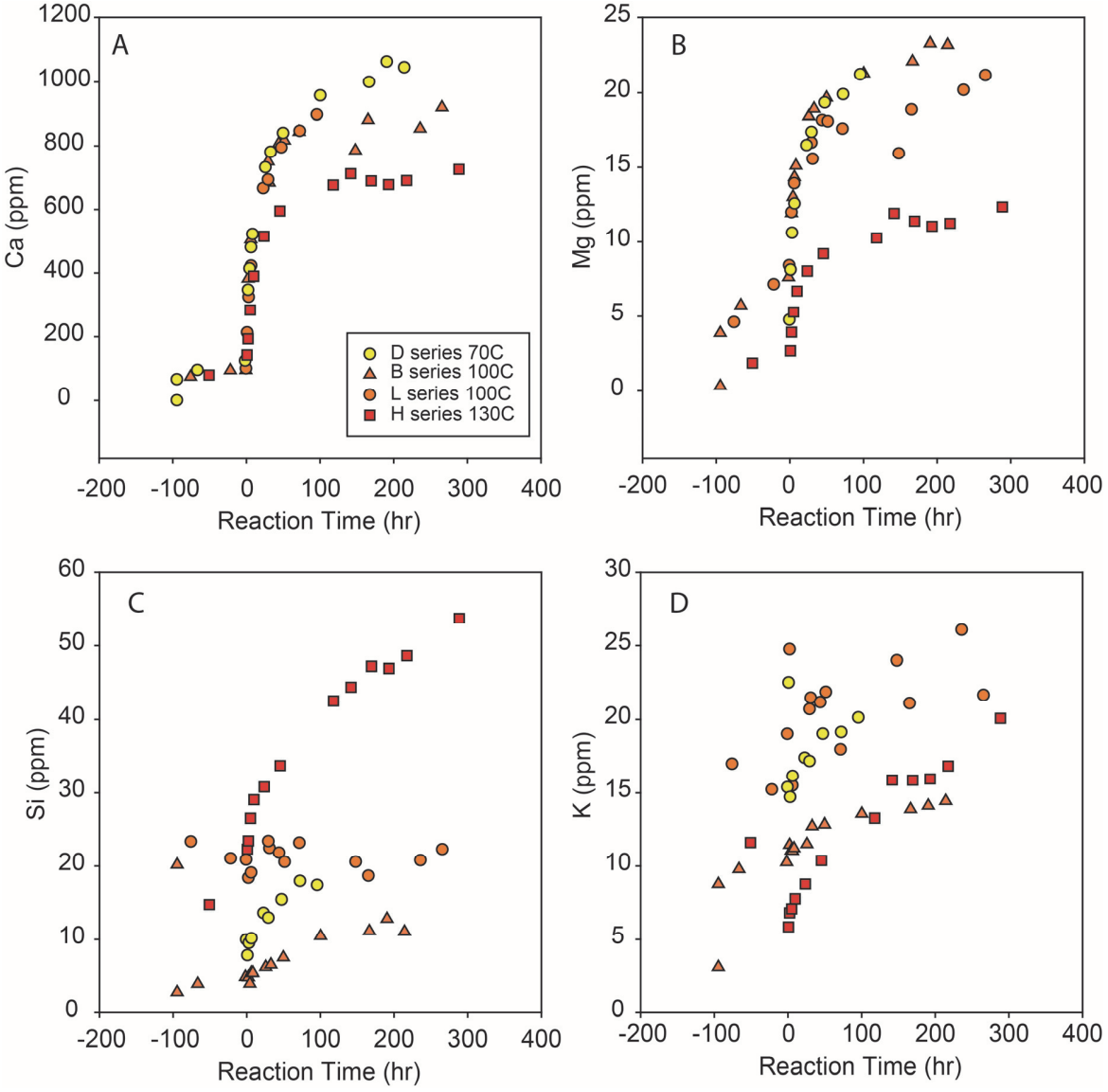

Fig. 1 Concentration of Ca, Mg, Si and K vs. reaction time with changing experimental temperature. The timing of increase for Ca and Mg show similar timing of concentration increase suggesting the same geochemical reaction is responsible for their increase in concentration. Si and K are similarly linked but since the timing of their concentration differs from the increase in Ca concentrations, another geochemical reaction is suggested. Also, there is an inverse relationship between temperature and Ca and Mg concentrations that does not exist in Si and K.

XRD results show small differences between the original and reacted sample. The reacted sample shows decreases in calcite and K-feldspar abundances and increases in Kaolinite and quartz (Table 1). For all minerals except quartz, changes are less than 2%, within the range of instrument error. Quartz abundance in the reacted sample is 5.6% higher than the unreacted sample which is higher than the experimental error.

Table 1. XRD mineral composition of the unreacted and reacted Miocene sample (Experiment B), Well Matagorda Island OCS-G-3733 A-6 (427034015800), 9205 ft.

Sample	Quartz	Kaolinite	Calcite	Illite	Plagioclase	K-feldspar	Total
Original	43.5	6.2	11.8	5.0	18.4	15.2	100.0
Reacted	49.1	4.5	9.6	5.1	18.1	13.6	100.0

SEM examination of unreacted samples shows that the majority of its calcite exists as fossils (mostly foraminifera) and calcite cement (Fig. 2). Fossil fragments, potassium feldspar and albite grains show dissolution on mineral surfaces. Carbonate cements usually show some smooth surfaces (Fig. 3).

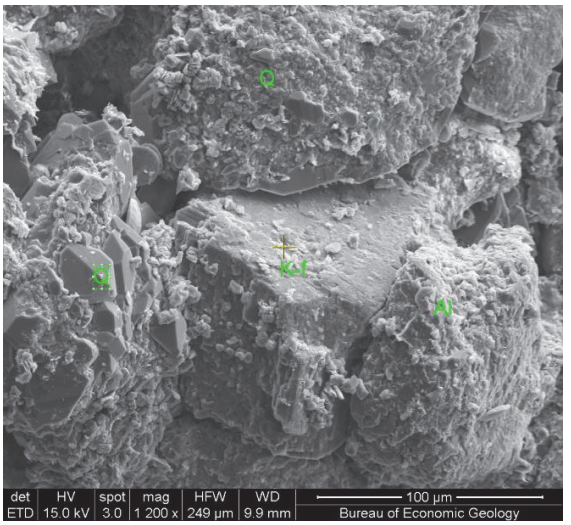

Fig. 2 SEM image of unreacted sample. Plagioclase (albite) (Al) and potassium feldspar (K-f) grains are usually blocky and sometimes show some corrosion features.

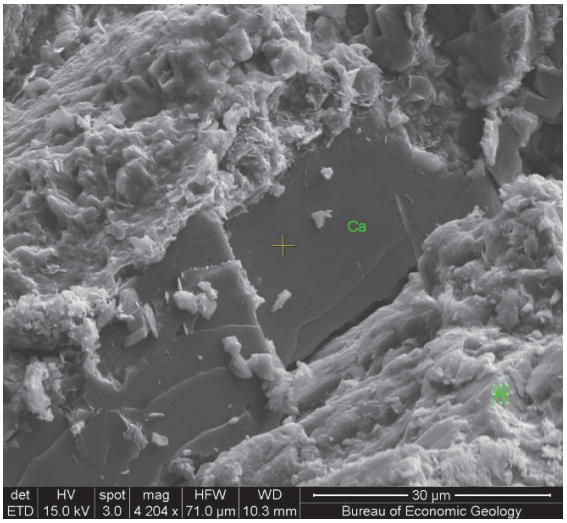

Fig. 3 Unreacted sample showing fresh un-weathered surfaces on calcite cements.

In post reaction SEM analysis potassium feldspar and plagioclase were heavily leached and corroded compared to the original sample (Fig. 4 and 5). However, it is difficult to completely separate the dissolution caused after $CO_{2(sc)}$ injection from that occurred during natural diagenesis and, therefore, to quantify dissolution amounts based only on SEM examination. Changes of water chemistry (increases of Na and K concentration) are more sensitive and can be used to calculate the amount of Feldspar dissolution. Also present near heavily weathered feldspar grains was books of kaolinite, a weathering product of feldspar (Fig. 5).
Amount of calcite dissolution is higher in the high salinity experiments compared to the DI water experiment. Calcite minerals were almost consumed at the reacted surface (below the mostly reacted surface calcite is still abundant). EDS scan results show that calcium content dropped from 4.7% to 0.6% at the reaction surface. More calcite was consumed in the brine experiments than in DI water experiment (Ca 1.1% at reacted surface). The SEM observation matches well with the water chemical analyses.

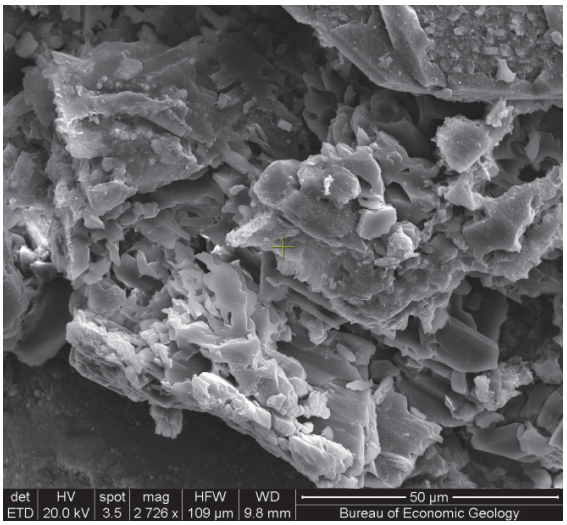

Fig. 4 SEM image of eroded plagioclase grain in a post reaction sample.

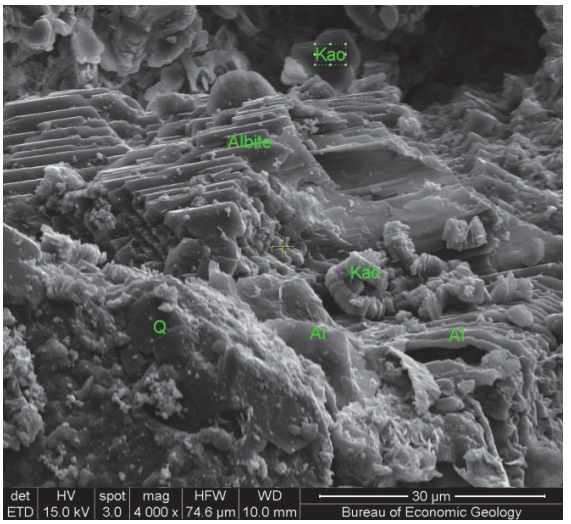

Fig. 5 SEM image of weathered albite grain in close association with kaolinite booklets (Kao) in a post reaction sample. Also shown in the image is a quartz grain.

Generally, the PHREEQC geochemical models reproduced the observed changes in elemental concentration after the reactive surface areas of the minerals that make up the rock samples identified in XRD analysis are quantified. A trial and error method was used to calibrate reactive surface area of minerals for each experiment by fitting concentrations of major ions from the PHREEQC models to the experimental results. The geochemical models were compared to the experimental results of Mg, Ca, K, Na, Si and Al (Fig. 6-8). Only the model results for Al differed significantly from the observed experimental results. Secondary minerals (Magnesite, Siderite, Ankerite and Dawsonite) that were not initially present in the rock samples, but whose precipitation was possible, were included in the model with a surface areas assumed to be 0.01 m^2. In the high salinity experiments the precipitation of Dawsonite was predicted by the PHREEQC model.

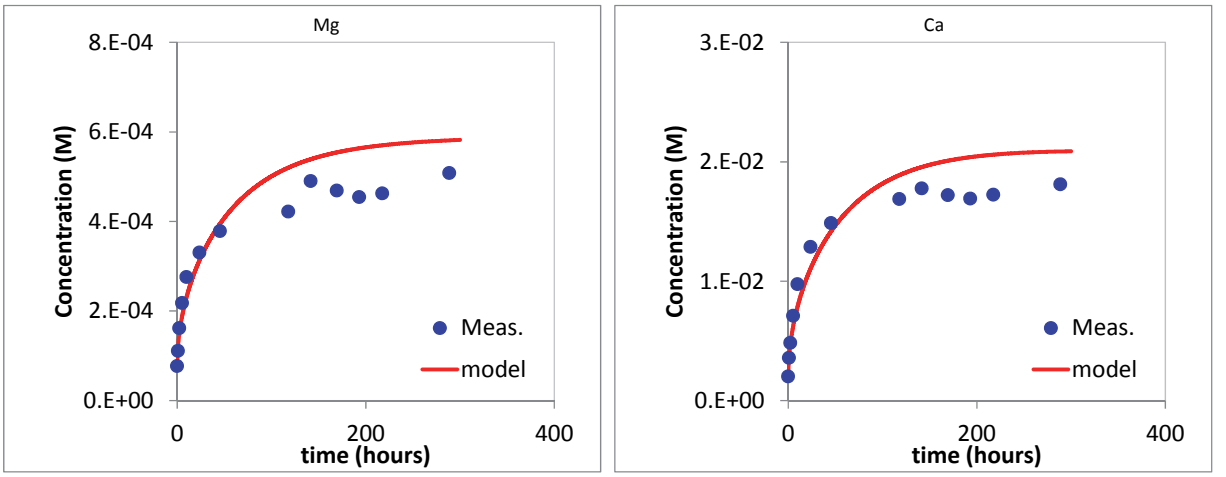

Fig. 6 Concentration of Mg and Ca vs. reaction time for the reaction at 130°C and 200 bar of pressure. Note the

similarity in the timing of increases in concentration which is likely controlled by carbonate dissolution.

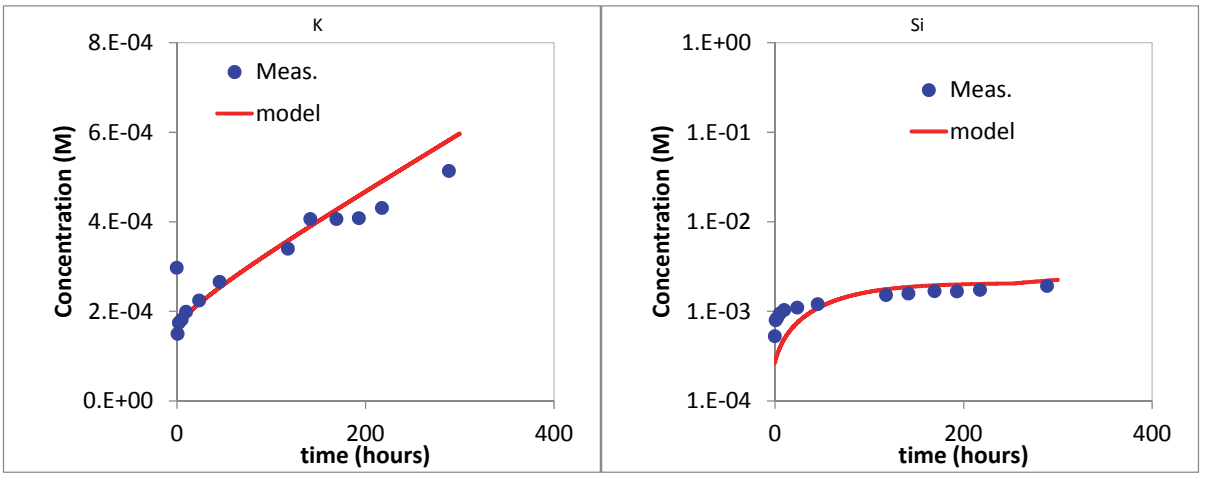

Fig. 7 Concentration of K and Si vs. reaction time for the reaction at 130°C and 200 bar of pressure. Note the timing of increases in concentrations are very different from the Ca and Mg plots suggesting a different geochemical reaction is controlling Si and K concentrations, most likely feldspar dissolution.

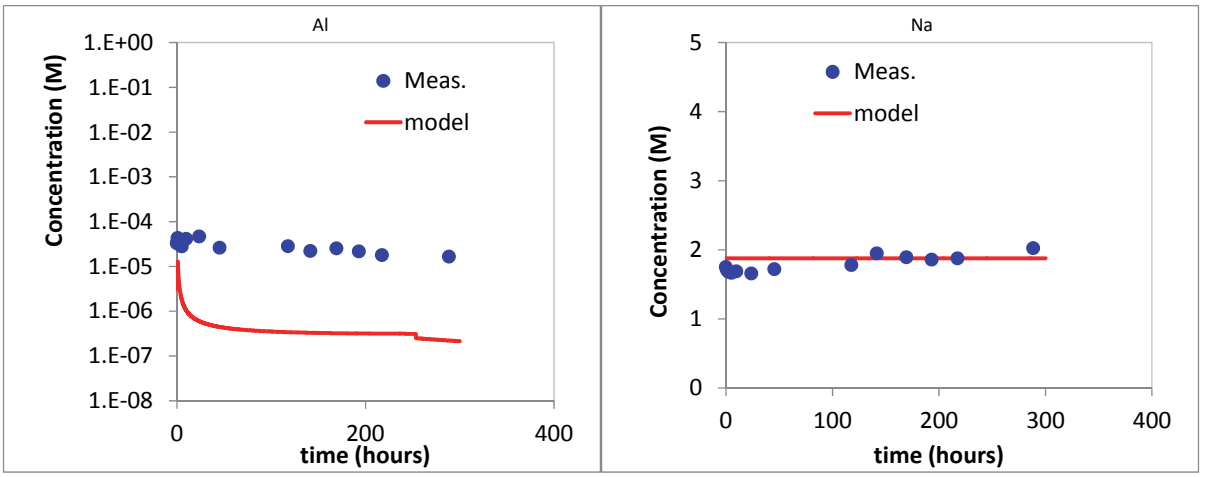

Fig. 8 Concentration of Al and Na vs. reaction time for the reaction at 130°C and 200 bar of pressure. Na concentrations were steady because geochemical reactions were not enough to affect the high NaCl salinity of the initial reaction fluid. Al concentrations did not fit the model results and Al was likely lost before analysis to an unidentified precipitate or sorption reactions.

Interpretation and conclusions

Combining the observations from 1) changes in elemental composition of reaction fluid during the reaction 2) SEM images of changes to mineral morphology and 3) XRD analysis showing subtle changes in mineral

abundance between pre and post reaction samples, one can conclude that two major mineral reactions occurred during the experiments. They are calcite dissolution (eq. 1) and K-feldspar and plagioclase dissolution (eq. 2) with calcite dissolution occurring at rates 1 to 2 orders of magnitude higher than feldspar dissolution.

$$CaCO_3 \text{ (Calcite)} + CO_2 + H_2O \rightarrow Ca^{2+} + 2HCO_3^- \quad (1)$$

$$2KAlSi_3O_8 \text{ (K-feldspar)} + 2H^+ + H_2O \rightarrow 2K^+ + Al_2Si_2O_5(OH)_4 \text{ (kaolinite)} + 4SiO_{2(aq)} \quad (2)$$

Calcite dissolution rate is dependent on the partial CO_2 pressure which is prominently controlled by reaction temperature. In the temperature range of this study, calcite dissolution rate decreases with higher reaction temperature. The calcite dissolution is not significantly altered by pressure variations. In fact, calcite dissolution rates at 200 bars and 300 bars are similar.

Plagioclase (albite) dissolution rate is as high as K-feldspar; therefore, dissolution of plagioclase may also have occurred during the experiment as modelling results suggested. The reaction experiment using DI water showed that Na concentrations in water increased from 24 ppm to 54 ppm during CO_2 stage. The additional sodium may indicate albite dissolution. In other experiments where 1.88 molar NaCl solutions were use, no notable Na increases were observed. The modest release of sodium from albite dissolution may have been swamped by high Na concentrations in background.

Kaolinite is a usual reaction product of feldspar dissolution (Eq.1). However, kaolinite XRD abundance in reacted sample is not higher than pre reaction samples; in fact it is lower than the original sample. XRD analysis of clay minerals usually has higher analytic errors because it is very difficult to achieve and control random orientation of clay minerals. Therefore, it is possible that small amount of kaolinite may have precipitated during the experiment, but XRD analysis is not sufficiently precise to detect its increase. Another possible explanation is that due to slow kinetic rate, kaolinite precipitation may be limited even it is supersaturated in the solution.

SEM analysis:

The reacted samples show a reaction rime of approximately 1 mm thick relative to the pre reaction samples. At the reacted surface, potassium feldspar and plagioclase (albite) grains apparently show more dissolution features than the unreacted sample. Kaolinite can often be seen in the vicinity of corroded feldspar grains, potentially a reaction product of feldspar dissolution. Most calcite was dissolved at the reaction surface and only a trace amount remained. It is difficult to completely separate the dissolution caused by CO_2 injection from that occurred during natural diagenesis and quantify it only based on SEM examination. Changes of water chemistry (increases of Na, Ca, Si and K concentration are more sensitive than visual observations and will be used to identify dissolution reactions.

The amount of calcite dissolution is higher in high salinity experiment compared to the DI experiment. Calcite minerals were almost completely consumed at the reacted surface (below the reacted surface calcite is still abundant). EDS scan results show that calcium content dropped from 4.7% in pre reaction sample to 0.6% in post reaction samples. The SEM observation matches well with the water chemical analyses. Calcite solubility is higher in the high salinity experiments than in the fresh water because the high Na concentrations of the brine increase the ion activity product of the solution which lower Ca activities and the calcite solubility product.

The geochemical models slightly overestimate Si concentration measurements and underestimate Al concentration measurements. Si and Al are dominated by dissolution-precipitation of silicate minerals and potential secondary minerals. Proper selection of secondary minerals in the geochemical model is important. Geochemical models show that Dawsonite precipitates in higher salinity (higher Na+ concentration) reactions.

herein do not necessarily state or reflect those of the United States Government or any agency thereof. This material is based upon work supported by the Department of Energy under Award NumberDE-FE0001941. In addition, the study was funded by the Texas General Land Office through GLO Contract No. 10-205-000-4100, which we gratefully acknowledge".

References

[1] Hepple, R. P. and Benson S. M. Geologic storage of carbon dioxide as a climate change mitigation strategy: performance requirements and the implications of surface seepage. Environmental Geology 2005; 47(4): 576-585.

[2] Hovorka, S. D., S. M. Benson, et al. Measuring permanence of CO_2 storage in saline formations; the Frio experiment. Environmental Geosciences 2006; 13(2): 105-121.

[3] Hillier, S. Accurate quantitative analysis of clay and other minerals in sandstones by XRD: comparison of a Rietveld and a reference intensity ratio (RIR) method and the importance of sample preparation. Clay Minerals 2000; 35: 291-302.

[4] Bish, D. L. Quantitative X-ray diffraction analysis of soils. Quantitative Methods in Soil Mineralogy: 1994; 267-295.

[5] Lu, J., M. Wilkinson, et al. Carbonate cements in Miller field of the UK North Sea: a natural analog for mineral trapping in CO2 geological storage. Environmental Earth Sciences 2011; 62(3): 507-517.

[6] Parkhurst, D. L. and C. A. J. Appelo User's guide to PHREEQC (version 2)--A computer program for speciation, batch-reaction, one-dimensional transport, and inverse geochemical calculations. U.S. Geological Survey Water-Resources Investigations Report 1999; 99-4259: 312.

[7] Berger, P. M., Roy, William R. and Mehnert, Edward Geochemical Modeling of Carbon Sequestration, MMV, and EOR in the Illinois Basin. Energy Procedia 2009; 1(1): 3437-3444.

[8] Heeschen, K., Risse, A., Ostertag-Henning, C., and Stadler, S. Importance of co-captured gases in the underground storage of CO2 : Quantification of mineral alterations in chemical experiments. Energy Procedia, 2011; 4, No., 4480-4486.

[9] Jacquemet, N., Le Gallo, Y., Estublier, A., Lachet, V., von Dalwigk, I., Yan, J., Azaroual, M., and Audigane, P. CO2 streams containing associated components--A review of the thermodynamic and geochemical properties and assessment of some reactive transport codes. Energy Procedia, 2009; 1, No. 1, 3739-3746.

[10] Koenen, M., Tambach, T. J., and Neele, F. P. Geochemical effects of impurities in CO2 on a sandstone reservoir. Energy Procedia, 2011; 4, No., 5343-5349.

[11] Soong, Y., Goodman, A. L., McCarthy-Jones, J. R., and Baltrus, J. P. Experimental and simulation studies on mineral trapping of CO2 with brine. Energy Conversion and Management, 2004; 45, No. 11-12, 1845-1859.

[12] Tarkowski, R. and Uliasz-Misiak, B. Reservoir rock reaction to CO2 - An experiment to estimate their use for carbon dioxide geological sequestration needs. Gospodarka Surowcami Mineralnymi-Mineral Resources Management, 2007;23, No. 3, 109-117.

[13] Xie, M., Bauer, S., Kolditz, O., Nowak, T., and Shao, H. Numerical simulation of reactive processes in an experiment with partially saturated bentonite. Journal of Contaminant Hydrology, 2006; 83, No. 1-2, 122-147.

[14] Johnson, J., Anderson, G., and Parkhurst, D., 2000, Database 'thermo.com.V8.R6.230,' Rev. 1.11. Lawrence Livermore National Lab, Livermore, Calif.

[15] CMG, 2011, WinProp User's Guide – Version 2011. Computer Modelling Group Ltd, Calgary.